

# Modification of the Inner Part of the Oil Palm Trunk (OPT) with Oil Palm Shell (OPS) Nanoparticles and Phenol Formaldehyde (PF) Resin: Physical, Mechanical, and Thermal Properties

Rudi Dungani,<sup>a,b</sup> Md Nazrul Islam,<sup>a,c</sup> H. P. S. Abdul Khalil,<sup>a,\*</sup> Y. Davoudpour,<sup>a</sup> and Alfi Rumidatul<sup>b</sup>

This study was conducted to enhance the physical, mechanical, and thermal properties of the inner part of the oil palm trunk (IP-OPT) impregnated with oil palm shell (OPS) nanoparticles at various concentrations (0, 1, 3, 5, and 10%) and phenol formaldehyde (PF) resin. The PF concentration was 15% (w/w basis) throughout the study. The physical, mechanical, and thermal properties of the OPS nanoparticle-impregnated IP-OPT lumber were analyzed according to various standards. It was found that IP-OPT gained a significant percentage of weight (up to 35.3%) due to the treatment, leading to a density increase from 0.42 to 0.89 g/cm<sup>3</sup>. The water absorption was reduced by up to 24%, which reduced the swelling coefficient, and thus, the anti-swelling efficiency was increased significantly. The tensile and flexural strengths increased from 9.77 to 19.64 MPa and from 14.46 to 38.55 MPa, respectively. The tensile and flexural moduli increased from 2.67 to 3.51 GPa and from 4.35 to 4.95 GPa, respectively, while the elongation at break decreased from 7.83 to 6.42%. The impact strength also increased significantly, from 6.90 to 15.85 kJ/m<sup>2</sup>. In addition, the thermal stability of IP-OPT was improved by the impregnation of OPS nanoparticles. Thus, it can be concluded that the impregnation of IP-OPT with OPS nanoparticles might be a good treatment process for enhancing the properties of the IP-OPT.

*Keywords:* Impregnation; Tensile; Flexural; SEM-EDX; TEM; XRD

*Contact information:* a: School of Industrial Technology, Universiti Sains Malaysia, 11800, Penang, Malaysia; b: School of Life Sciences and Technology, Institut Teknologi Bandung, Gedung Labtex XI, Jalan Ganessa 10, Bandung 40132, West Java-Indonesia; c: School of Life Science, Khulna University, Khulna 9208, Bangladesh; \*Corresponding author: akhalilhps@gmail.com

## INTRODUCTION

The development of the palm oil industries throughout Malaysia is one of the most successful stories in the history of the country's agricultural sector (Mahlia *et al.* 2001). Due to global oil and fat demands and the increased use of palm oil in food-related industries, there are large oil palm plantations all over Malaysia. Malaysia is the second largest producer after Indonesia and is the world's largest crude palm oil exporter. An oil palm tree reaches an average volume of 1.638 m<sup>3</sup> after its commercial life span (Bakar *et al.* 1998); therefore, more than 20 million m<sup>3</sup> of biomass from oil palm trunk (OPT) are available annually in Malaysia alone. This is a spectacular amount of natural solid agricultural waste that has the potential for use as biomass resources for products such as fibre and cellulose, as well as raw material to be substituted for wood material from

natural forests for furniture and building materials. The advantages of OPT are its abundance, low cost, and low density, as well as being safe to handle, renewable, economically feasible, and biodegradable (Dungani *et al.* 2013a,b; Islam *et al.* 2013); however, it suffers from some drawbacks such as being dimensionally unstable and having lower strength, less durability, and lower machining properties (Abdul Khalil *et al.* 2012, 2010; Bhat and Abdul Khalil 2011; Bhat *et al.* 2010) than some other woods. According to Baker *et al.* (1999a, b, 1998), OPT has very low dimensional stability with high shrinkage, low strength (class III-V), and low durability (class V). The inner part is more sawable than the outer part. Several researchers (Hartono 2012; Erwinsyah 2008; Bakar *et al.* 1999a, 1998; Lim and Khoo 1986; Killmann and Choon 1985) conducted their studies with the outer part of the OPT and concluded that only one-third of the diameter and three-fourths of the height could be used for light-weight building materials and furniture construction because of its physical and mechanical properties. The remaining biomass has very limited to no use. The addition of polymeric resin improves the properties (Abdul Khalil *et al.* 2012, 2010; Bhat *et al.* 2010; Abdullah 2010); however, the IP-OPT remains still far away from achieving the properties suitable for building materials and furniture construction.

Nanomaterials have recently attracted scientific and industrial interest due to their low density, high mechanical properties, and many other improved properties. Nanocomposite materials consisting of a polymeric matrix and nanoparticles have many uses. Nanocomposites exhibit superior property enhancements with lower filler contents compared to conventional micro and macro or neat counterparts (Zhang *et al.* 2011). This property enhancement can be further improved by adding a variety of nanoparticles and resins to composite materials. Oil palm shell (OPS) is also an oil palm biomass that has little or no use. Nanoparticles can be produced from the OPS, as mentioned in earlier studies (Shafiqh *et al.* 2011; Arami-Niya *et al.* 2010; Paul *et al.* 2007). Biodegradability and renewability are the added advantages of this type of nanoparticle.

Thus, this study was conducted to impregnate IP-OPT with OPS nanoparticles and phenol formaldehyde resin to enhance the physical, mechanical, and thermal properties of the IP-OPT. The principal idea behind this process is that the OPS nanoparticles in the cell lumen may reinforce the thermosetting resin matrix by linking with the OPT cell wall. The effect of OPS nanoparticle loading on the physical, mechanical, and thermal properties of IP-OPT was studied.

## EXPERIMENTAL

### Materials

*Preparation of the inner part of oil palm trunk (IP-OPT) samples and oil palm shell (OPS) nanoparticles*

Commercially available OPT from the bottom portion of the trunk was sawn into pieces of square lumber with sides of 150 mm and then dried in a kiln to a moisture content of 13 to 15%. The dried square lumber was then cut into 50 mm x 50 mm x 500 mm segments from the inner two-thirds of the diameter for use in the experiments. The average density of the inner part of the sample was 0.29 g/cm<sup>3</sup>. At least 180 samples were prepared for one experiment.

Oil palm shell (OPS) was collected from a palm-oil processing mill in Banten, Indonesia, in the form of chips. The OPS chips were ground using a grinder/refiner to

produce powder, and the powder was dried to a total evaporable moisture content of 1.5%. Nanoparticles were prepared from these OPS chips by high-energy ball milling (Pulverisette, Fritsch, Germany) for 30 h with a rotation speed of 170 rpm. The milling chamber was made of tungsten carbide, and the balls were stainless steel with diameters of 10 mm. Toluene was used to avoid agglomeration, as reported by Paul *et al.* (2007).

Phenol formaldehyde (PF) resin was used to impregnate OPS nanoparticles into the OPT lumen. The PF resin was collected from the Palmolite Adhesive Company, Indonesia. The properties of the PF resin are shown in Table 1.

**Table 1.** Properties of PF Resin

Resin properties	Value
Viscosity @ 25 °C (poise)	2.27
Specific Gravity @ 25 °C	1.200
Resin Content @135 °C (%)	42.5
pH (meter/25 °C)	12.45
Molecular weight (Mn)	4000

## Methods

### *Impregnation of nanoparticles into IP-OPT*

Phenol-formaldehyde (PF) resin was prepared at high molecular weight with a concentration of 15% w/w. Exactly 1, 3, 5, and 10% w/w OPS nanoparticles with diameters ranging from 50 to 100 nm were added to the PF resin to obtain different concentrations. The mixtures (PF resin and OPS nanofiller) were compounded using a twin-screw extruder (Haake Model Rheodrive 500) and added to the chamber for impregnating the IP-OPT. The mixture was incorporated into the chamber to begin the process of impregnation. The PF-OPS nanoparticle mixture was impregnated into the IP-OPT using a vacuum-pressure method with the schedule shown in Fig. 1. The impregnated IP-OPT samples were incubated in an oven for 3 h at 150 °C for curing to remove excess resin.

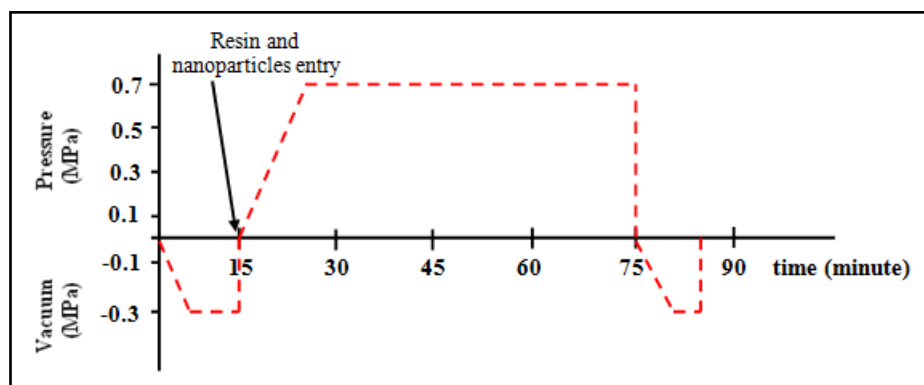


**Fig. 1.** Impregnation process with time and pressure

### *Characterization of OPS nanoparticles impregnated into IP-OPT*

The OPS nanoparticles were analyzed with a scanning electron microscope (SEM) (ZEISS type EVO 50, Germany) with energy dispersive X-ray (EDX) (Leica Cambridge S-360, Germany), transmission electron microscope (TEM) (Philips CM12 Instrument, Germany), and X-ray diffraction (XRD) (PHILIPS PW 1050 X-pert, Germany) to determine their structure, morphology, and crystallinity index. The average

particle size was determined from the X-ray diffraction peaks using equation Scherrer's Equation (Patterson 1939):

$$D = K\lambda/\beta\cos\theta \quad (1)$$

where  $D$  is the particle diameter,  $\lambda$  is the X-Ray wavelength,  $\beta$  is the full width at half maximum (FWHM) of the diffraction peak,  $\theta$  is the diffraction angle, and  $K$  is the Scherrer's constant of the order of unity for usual crystals.

#### *Determination of physical properties*

Weight gain percentage, density, dimensional stability, and water absorption were calculated using the following equations:

$$\text{Weight gain (WG) (\%)} = \{(m_a - m_b)/m_b\} \times 100 \quad (2)$$

where  $m_a$  = the mass of the sample after impregnation (g) and  $m_b$  = the mass of the sample before impregnation (g);

$$\text{Density (p) (g/cm}^3\text{)} = m_o/V_g \quad (3)$$

where  $m_o$  = the mass of oven dry sample (g) and  $V_g$  = the initial volume of sample (cm<sup>3</sup>);

$$\text{Volumetric swelling coefficient (SC) (\%)} = \{(V_2 - V_1)/V_1\} \times 100 \quad (4)$$

where  $V_2$  = the volume of the saturated sample (cm<sup>3</sup>) and  $V_1$  = the volume of the oven dried sample (cm<sup>3</sup>);

$$\text{Antiswelling efficiency (ASE) (\%)} = \{(S_u - S_m)/S_u\} \times 100 \quad (5)$$

where  $S_u$  and  $S_m$  are the swelling coefficients of untreated and treated IP-OPT, respectively; and

$$\text{Water absorption, WA (\%)} = \{(m_2 - m_1)/m_1\} \times 100 \quad (6)$$

where  $m_1$  = the mass of the sample before soaking (g), and  $m_2$  = the mass of the sample after soaking of the impregnated samples in distilled water for 24 h.

#### *Determination of mechanical properties*

*Tensile test:* Tensile strength, modulus, and elongation at break were determined according to ASTM–D3039 using a universal testing machine (Instron Model 5582).

*Flexural test:* Flexural strength and modulus were determined according to ASTM D790 using a universal testing machine (Instron Model 5582).

*Impact strength test:* The charpy impact test was performed according to ASTM D256 using a geotech testing machine (Model GT-7045 MD, Impact Pendulum Tester Zwick). The widths and thicknesses of the unnotched samples were measured and recorded.

#### *Determination of thermal properties*

*Thermogravimetric analysis:* Thermogravimetric analysis (TGA) was carried out on a Perkin Elmer (TGA-6) analyzer with a heating rate of 20 °C/min with a temperature range between 27 and 900 °C for complete thermal degradation.

#### *Data analysis*

Univariate analyses of variance (ANOVA) were performed with linear models in a completely randomized design (CRD) using SPSS version 16.0.

## RESULTS AND DISCUSSION

### Characterization of OPS Nanoparticles

Figure 2 shows the OPS nanoparticles. Typically, nano-structured OPS consist of irregular and crushed shapes, indicating their nanometric nature. The SEM study of OPS nanoparticles showed that there was agglomeration of particles. Raw OPS is highly porous, with sufficiently high solid densities, having angular and irregularly shaped components, although cellular texture has also been reported (Guo and Lua 2002). The TEM micrograph confirmed that the average OPS particle size ranged between 50 and 100 nm (Fig. 3).

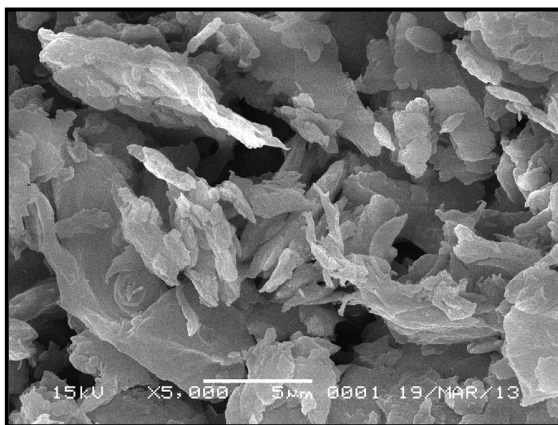


**Fig. 2.** SEM micrograph of OPS nanoparticles (5000x magnification)

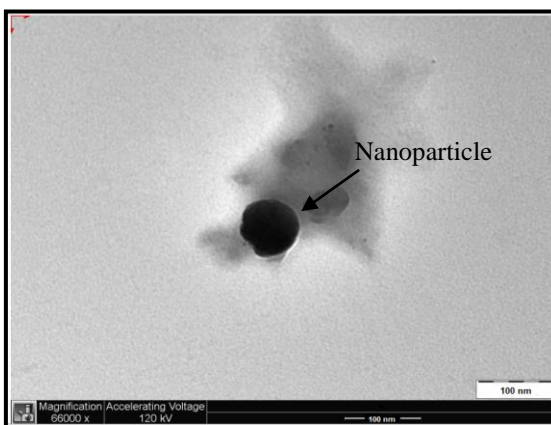


**Fig. 3.** TEM micrograph of OPS nanoparticles

The crystallinity index of the OPS nanoparticles was 15.2%; thus, the amorphous region increased in the nanoparticles (84.8%) (Fig. 4), as previously reported by Lai and Idris (2013) for different parts of oil palm plants.

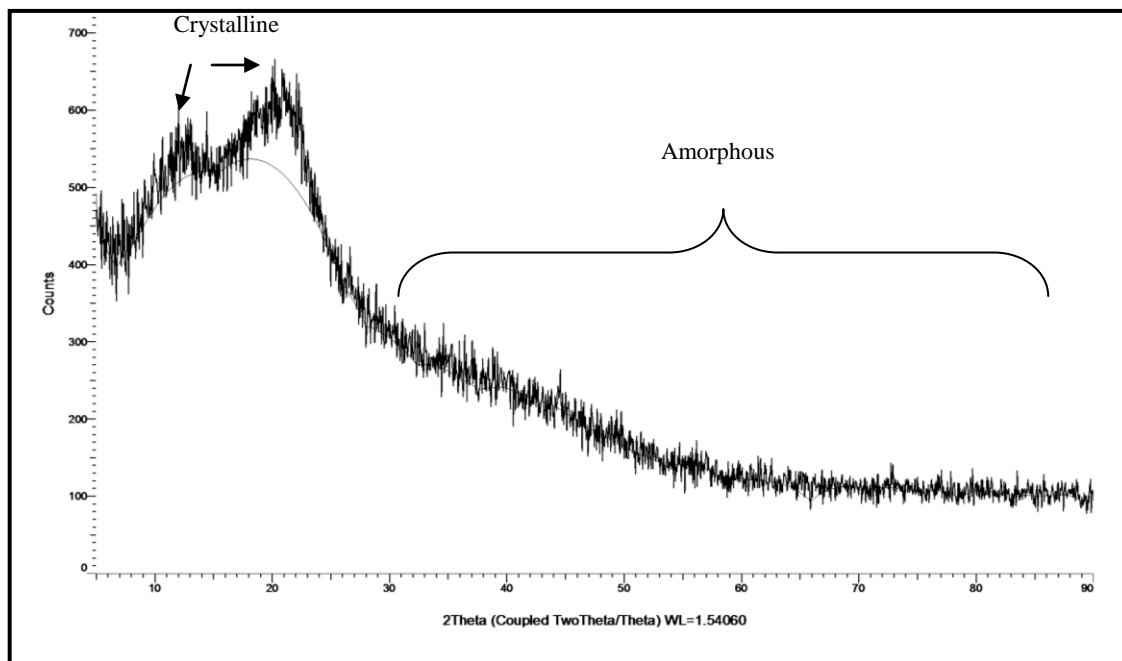


**Fig. 4.** XRD spectrum of OPS

Park *et al.* (2010) reported that higher crystallinity index increased the hardness and decreased the transparency and diffusion by increasing the density of the materials; thus, particles having low crystallinity are suitable for impregnation and use as reinforcing materials. Hence, the low crystallinity index of OPS nanoparticles was advantageous for impregnation into OPT with PF resin as an effective reinforcement in the polymer matrix. This interpretation was confirmed by the EDX spectroscopy shown in Fig. 5, where silica was not found in the OPS nanoparticles; however, the silica content was very high for oil palm ash as were reported by other researchers, who found 40% silica (Zainudin *et al.* 2005) and 25% silica (Abdul Khalil *et al.* 2011).

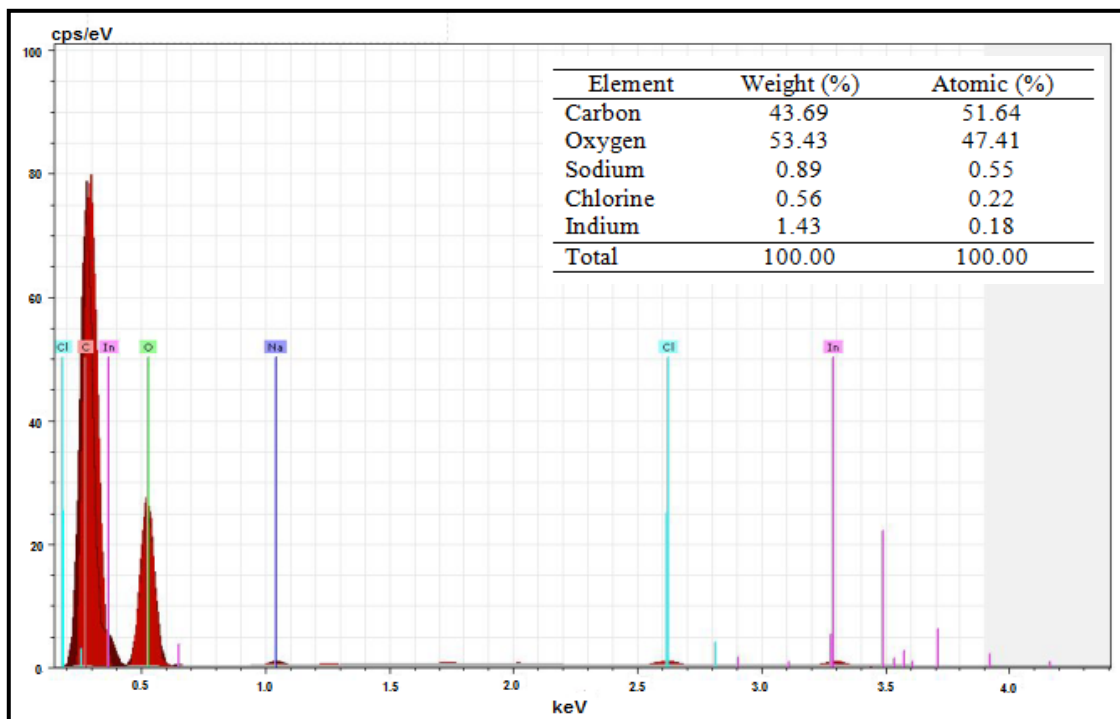


Fig. 5. EDX spectrum of OPS

### Physical Properties of OPS Nanoparticle-Impregnated OPT

The weight gain percentage (WGP) of IP-OPT after OPS nanoparticle impregnation with PF resin at various nanoparticle concentrations is shown in Fig. 6. The OPS nanoparticles and PF resin significantly increased the weight of IP-OPT. This weight gain was linear with nanoparticle concentration up to 5%. No significant increment ( $\alpha = 0.05$ ) for weight gain was found when the OPS nanoparticle concentration was changed from 5 to 10%. PF resin having higher molecular weight penetrates only into the cell lumen and has the tendency to leach out from the cell lumen, causing the loss of the cell bulking effect (Ibach and Ellis 2005). The use of nanoparticles prevents the leaching of the resin from the cell lumen by immediate polymerization and fixation after impregnation. The permeability of dried OPT is very high, which might be the reason for this higher WGP. Dried OPT has very high porosity, and its parenchyma tissue behaves like a sponge that can easily absorb resin. These properties of dried OPT enable better impregnation, which leads to an increase in resin loading (Bhat *et al.* 2010).

The impregnated PF resin and OPS nanoparticles as were seen on a freshly cut cross-section increased the density of IP-OPT significantly ( $\alpha = 0.05$ ). Figure 6 shows the

change in density of IP-OPT with the impregnation of PF resin. The untreated IP-OPT density ( $0.29 \text{ g/cm}^3$ ) increased to  $0.42 \text{ g/cm}^3$  after impregnation of only PF resin. This density reached its maximum ( $0.89 \text{ g/cm}^3$ ) when 5% OPS nanoparticles with PF resin were impregnated into the IP-OPT. Ten percent addition of OPS nanoparticles with PF resin increased the density of the mixture, which hindered the penetration of liquid into the IP-OPT during the treatment. This might be the cause of the lower density and weight gain percentage of the IP-OPT when treated with 10% OPS nanoparticles. PF resin improved the density of IP-OPT, which was further enhanced by the addition of OPS nanoparticles. However, lower WGP sometimes does not change the density (Deka *et al.* 2003).

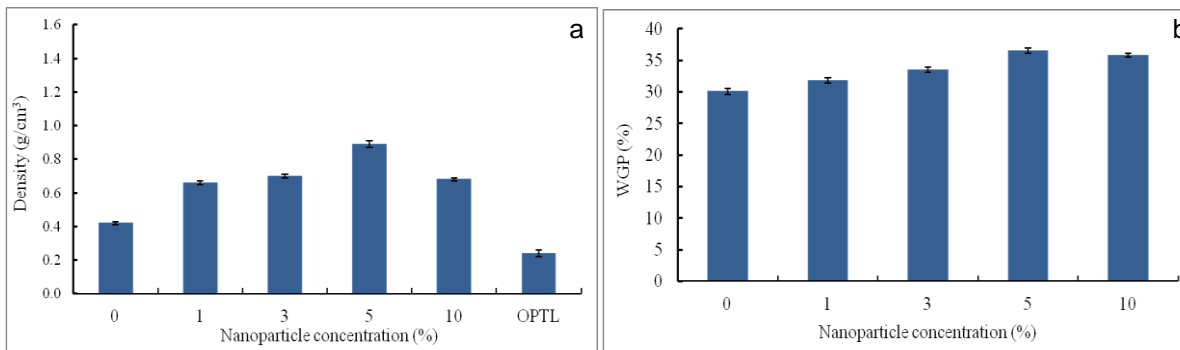


**Fig. 6.** (a) Density, and (b) WGP of IP-OPT impregnated with PF resin and OPS nanoparticles at various nanoparticle concentrations

The increase in WGP and density might be due to the bulking effect of the cell lumen where crystallization of the nanoparticles occurred between cell wall and the resin matrix, which was fused by resin curing. The density may have increased because of the increase of polymer content in the wood.

Significant differences ( $\alpha = 0.05$ ) for water absorption were found between treated and untreated samples. PF resin impregnation reduced the water absorption, which was further decreased with the addition of OPS nanoparticles (Fig. 7). The reduction of the water absorption by the IP-OPT due to the treatment would automatically improve some other physical properties. There was no significant difference ( $\alpha = 0.05$ ) in water absorption between different nanoparticle concentrations, though it was slightly higher for 1 and 10% OPS nanoparticle concentrations. The presence of a higher amount of hydrophilic OPS nanoparticles in the cell lumen might influence the WA for the 10% OPS nanoparticle concentration. The highest water absorption was found in dried OPT. These results were similar to the results reported by Abdullah (2010), which were also supported by Amin and Abdul Khalil (2004). They stated that dried OPT contained higher amounts of parenchyma tissue, which leads to higher absorption of water compared to the vascular bundles.

Impregnation of PF resin and OPS nanoparticles further improved the physical properties of the IP-OPT, which was evident from the reduction of the swelling coefficient (SC) (Fig. 7). Chen *et al.* (2009) reported that water molecules held in the cell lumen by surface tension and force of capillary action subsequently penetrated into the cell wall, resulting in the swelling of cells, although the amount of swelling depends on the amount of impregnating liquids. The PF resin and OPS nanoparticles effectively served as a barrier against the diffusion of water molecules into the cell wall and cell lumen or at least reduced the permeability behavior of the fibres by blocking the cell

lumen and micropores of cells. The SC reduced as the concentration of nanofiller increased, and the lowest SC was observed for the 5% OPS nanoparticle concentration.

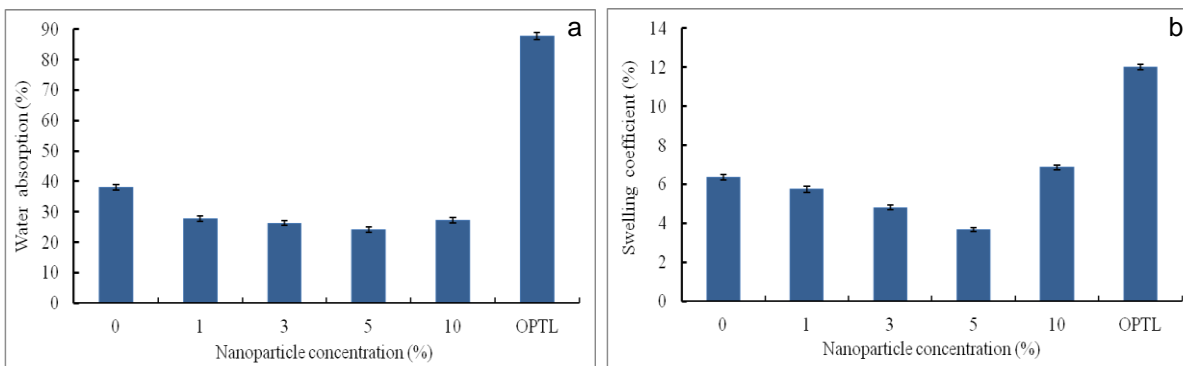


**Fig. 7.** (a) Water absorption, and (b) swelling coefficient of IP-OPT impregnated with PF resin and OPS nanoparticles at various nanoparticle concentrations

As expected, the IP-OPT absorbed a high amount of moisture. Figure 8a shows the variability in size and shape of the cell wall structures of the IP-OPT. The thin cell wall and large lumens may have been the cause of this high water absorption, as reported by Erwinsyah (2008) and Abdul Khalil *et al.* (2008). The hydrophilic properties of the OPT due to the formation of hydrogen bonds between the hydroxyl groups and water molecules may be another reason for the higher WA (Dungani *et al.* 2013a, b; Bhat *et al.* 2010; Hu *et al.* 2010; Islam *et al.* 2010). This study clearly showed that WA and the formation of hydrogen bonds were discontinued by enclosing the OPT cells with hydrophobic polymer resin and OPS nanoparticles. The OPT samples became moisture-resistant by the polymerization of the cured resin, which expelled moisture from the OPT cells. This phenomenon can be clearly understood by observing the SEM micrographs obtained after impregnating the IP-OPT with OPS nanoparticles and PF resin (Fig. 8b). The SEM micrograph shows that the cell walls and cell lumens are encrusted with the PF resin and OPS nanoparticles, which prohibited the absorption and penetration of water into cells.

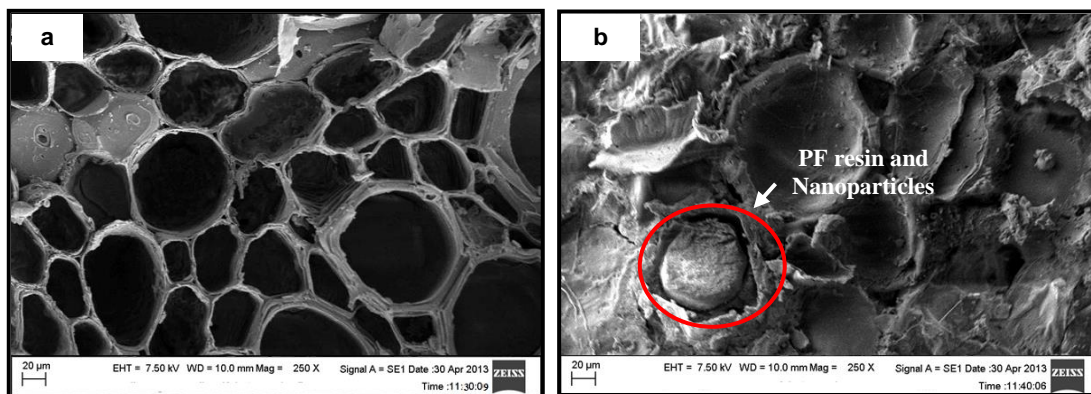


**Fig. 8.** SEM micrographs of IP-OPT at transverse section (250x magnification) (a) before, and (b) after PF resin and OPS nanoparticles impregnation

Figure 9 shows the relationship between ASE and nanoparticle concentrations. ASE increased with increasing nanoparticle concentration up to 5%, and then decreased with further increases of the nanoparticle concentrations. The highest OPS nanoparticle

concentration (10%) may induce the formation of checks in the cell lumen during treatment, which could be the reason for the ASE reduction. Impregnation with OPS nanoparticles and PF resin caused a bulking of the cells, which decreased additional water swelling. An increase in ASE values at high WGP may have been due to resin and nanoparticle loading, which increased the density and reduced the porosity, resulting in lower dimensional changes of OPT samples. Thus, volumetric shrinkage decreased, and the formation of wall polymers inside the cell wall enhanced the dimensional stability of the OPT (Bhat *et al.* 2010).

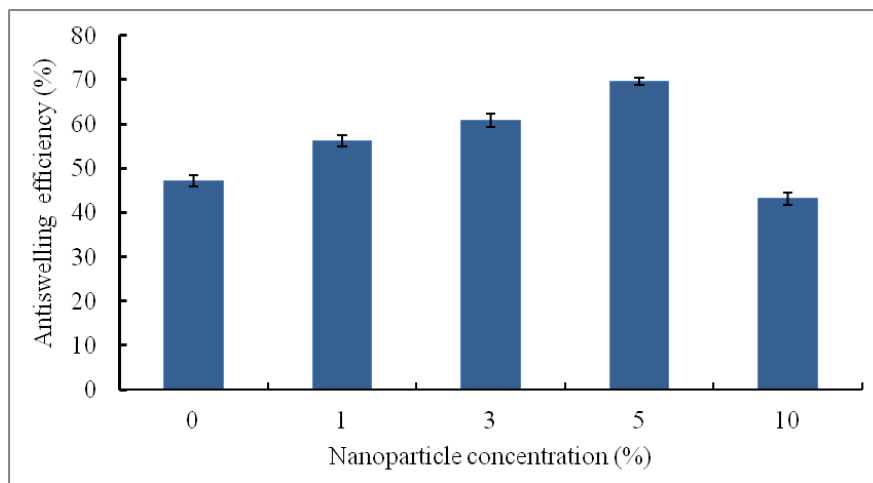


**Fig. 9.** Antiswelling efficiency of IP-OPT impregnated with PF resin and OPS nanoparticles at various nanoparticle concentrations

### Mechanical Properties of PF-NF-Impregnated IP-OPT

The tensile strength and tensile modulus increased (Fig. 10), while elongation at break decreased (Fig. 11), due to the impregnation of OPS nanoparticles into the IP-OPT. The highest tensile strength was found at 5% OPS nanoparticle impregnation (19.6 MPa), while impregnation with PF resin alone showed comparatively lower tensile strength (9.8 MPa). Thus, OPS nanoparticles not only improved the physical properties but also increased the tensile strength of the IP-OPT.

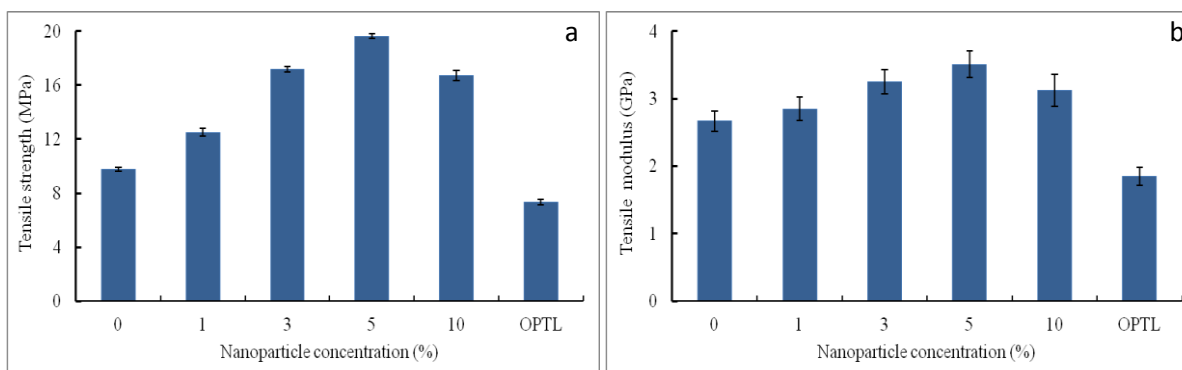


**Fig. 10.** (a) Tensile strength, and (b) tensile modulus of IP-OPT impregnated with PF resin and OPS nanoparticles at various nanoparticle concentrations

Because more added substances (PF resin and OPS nanoparticles) in the IP-OPT provided more area to resist stress, a stronger IP-OPT was formed compared to the

control sample. This was due to the fact that OPT samples absorbed PF resin and OPS nanoparticles, which react to stress, resulting in an increase in tensile strength. Similar findings have been reported by many researchers (Abdul Khalil *et al.* 2012, 2010; Anwar *et al.* 2009; Deka and Saikia 2000), who mentioned that resin impregnation improved the strength of several lignocellulosic materials.

The increase in the tensile strength of fibres can also be explained by the reduction of the moisture content. When the fibres absorb moisture and diffuse it into the cell wall, the water molecules start to form hydrogen bonds with the hydroxyl groups of the fibres, and cellulose chains move apart, resulting in an increase in microfibril size. This causes a change in cell wall size, which in turn causes the fibres to swell. As the cellulose inside the fibres moves farther apart due to swelling, large gaps created between the cellulose chains weaken the inter- and intramolecular bonding of fibres. The decrease in strength of natural fibres due to the presence of moisture has been reported by several researchers (Bhat *et al.* 2010; Abdul Khalil *et al.* 2010; Mizanur Rahman 2009; Dhakal *et al.* 2007; Joseph *et al.* 2002). Mishra *et al.* (2001) mentioned that the strength of pineapple leaf fibre (PALF) decreases up to 50% when tested under wet conditions.

The resin that was locked in the fibre caused the fibre to become more rigid and stiff, resulting in fibre brittleness. Figure 11a-b shows the presence of PF resin and OPS nanoparticles in the parenchyma cells. It is clear that impregnation with PF resin and OPS nanoparticles significantly ( $\alpha = 0.05$ ) reduced the porosity of OPT compared to the control.

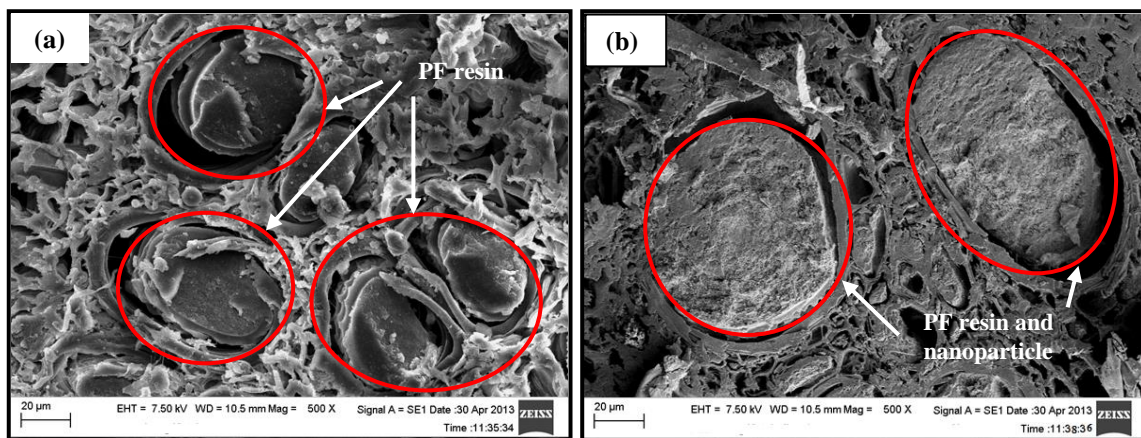


**Fig. 11.** SEM micrographs of IP-OPT showing parenchyma at transverse section (500x magnification) impregnated with (a) PF, and (b) PF resin and OPS nanoparticles

The elongation at break of OPT impregnated with PF resin and OPS nanoparticles was reduced with increasing OPS nanoparticle concentrations (Fig. 12). The lowest elongation at break was found when the OPS nanoparticle concentration was 5%. It was expected that the penetration of OPS nanoparticles would be higher when the concentration of nanoparticles was also higher. However, this assumption was incorrect according to Fig. 6, where the WGP and density were higher for the 5% OPS nanoparticle concentration. It can be seen in Fig. 12 that higher PF resin and OPS nanoparticle concentrations increased the brittleness and showed lower elongation at break compared to impregnation with PF resin alone. Abdul Khalil *et al.* (2001) also found similar results and mentioned that higher WGP increased the brittleness and ultimately lowered the values for elongation at break.

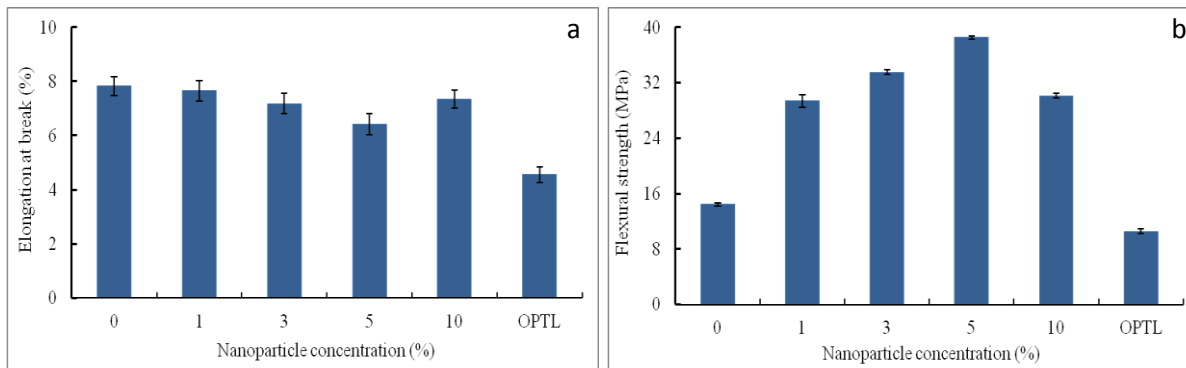


**Fig. 12.** (a) Elongation at break, and (b) flexural strength of IP-OPT impregnated with PF resin and OPS nanoparticles at various nanoparticle concentrations

The flexural properties increased with increasing OPS nanoparticle concentrations up to 5%; however, the flexural strength decreased for the 10% OPS nanoparticle concentration (Figs. 12 and 13). The higher OPS nanoparticle concentration (10%) increased the density of the impregnated liquid, which may have prohibited its penetration into the IP-OPT. Similar to other properties, the flexural strength and flexural modulus were also higher (38.5 MPa and 5.0 GPa, respectively) when the OPS nanoparticle concentration was 5%. However, the flexural properties decreased when the nanoparticle concentration exceeded 5%. The high polarity of PF resin helps to form strong hydrogen bonds with the hydroxyl groups (Mishra *et al.* 2000), which increases the flexural properties; however, cell walls have been shown to collapse due to the presence of OPS nanoparticles (Abdul Khalil *et al.* 2010). These two contradictory functions of PF resin and OPS nanoparticles might be responsible for these lower flexural properties with higher OPS nanoparticle concentrations.

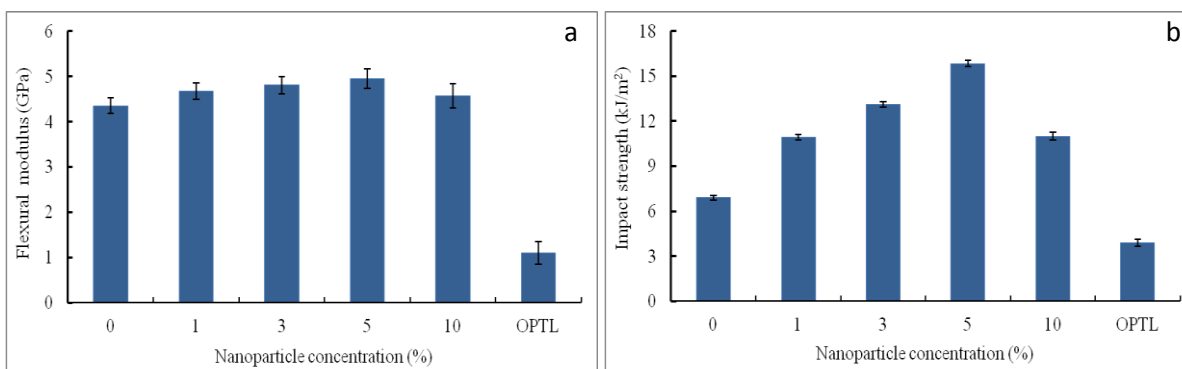


**Fig. 13.** (a) Flexural modulus, and (b) impact strength of IP-OPT impregnated with PF resin and OPS nanoparticles at various nanoparticle concentrations

The impact properties are directly related to the interfacial bond strength, matrix and fibre properties (Abdul Khalil and Rozman 2004). Figure 13 shows the impact strength of OPS nanoparticle-impregnated IP-OPT. Similar to other properties, the impact strength increased with increasing OPS nanoparticle concentration up to 5%. This is because of the fibre-matrix bonding (Bhat *et al.* 2010; Abdul Khalil *et al.* 2010; Bakar *et al.* 2008). Higher interfacial interaction between the fibres and matrix at 5% OPS

nanoparticle concentration was related to the greater impregnation of OPS nanoparticles into pits and/or pores of IP-OPT, thereby enhancing its impact properties.

According to Brown (1980) and Seena *et al.* (2002), extra energy is needed to form bonds between filler and matrix, suggesting that the impact failure of the composite may be caused by matrix fracture, fibre/matrix bonding, and fibre pull-out. With 5% OPS nanoparticle concentration, greater impregnation of PF resin and OPS nanoparticles into pits and pores of the OPT samples may have led to higher impact properties. Therefore, nanoparticle concentrations beyond 5% increased brittleness, and the composites thus could not efficiently resist fracturing under stress applied at high speeds. This phenomenon may also have been a result of the effective stress transfer between the strongly adherent filler and matrix due to physical and chemical bonding (Leong *et al.* 2004).

### Thermal Properties of PF-NF-Impregnated TP-OTP

The TGA curves showed a slight weight loss below 100 °C, which can be attributed to the evaporation of water. The weight loss ranged between 6.4 and 7.5%, in which the impregnated samples with 5% OPS nanoparticle concentration showed the lowest value (Fig. 14). The TGA curve showed that IP-OPT impregnated with higher OPS nanoparticle concentrations was more thermally stable compared to those with lower OPS nanoparticles concentrations. This is quite normal, as higher OPS nanoparticle concentrations can result in impregnation of a larger amount of material, which make the structure more thermally stable. Similar findings have also been reported by Bhat *et al.* (2010), in which the quantity of chemical components in the samples affects the thermal stability and degradation.

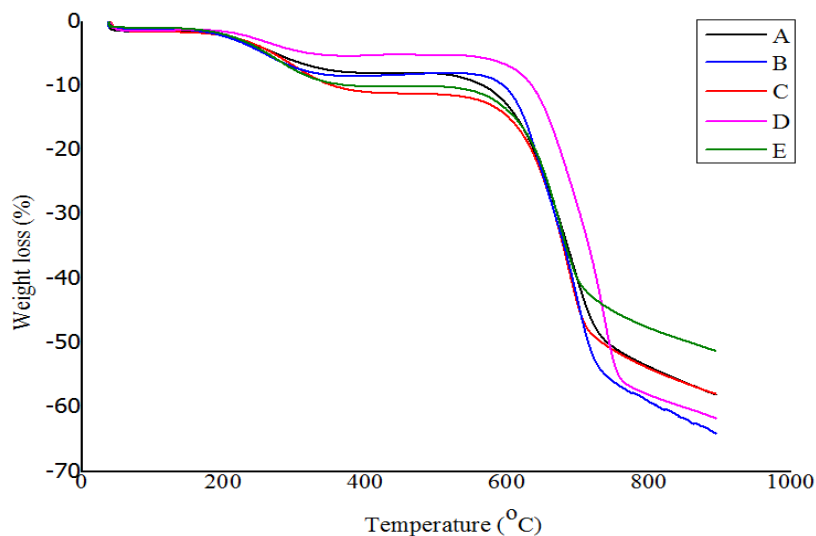


**Fig. 14.** Thermogravimetric analysis (TGA) curves for IP-OPT after impregnation of OPS at different concentrations (A) 0%, (B) 1%, (C) 3%, (D) 5%, and (E) 10%.

Degradation of the dried OPT samples occurred at 315 °C to 390 °C. Yang *et al.* (2004) found similar results, in which thermal degradation of oil palm waste started at approximately 220 °C, with lignin pyrolysis occurring from 300 °C to 340°C. Meanwhile, the total weight losses (%) at the final temperature of 900 °C were 42.1, 42.3, 44.2, 52.580, and 49.1% for OPS nanoparticle concentrations of 0, 1, 3, 5, and 10%, respectively. The weight loss at this temperature region (above 900 °C) corresponded to

the formation of volatile products that arose from random chain scission and inter-molecular transfer involving tertiary hydrogen abstractions from hemicellulose, cellulose, and lignin (Remiro *et al.* 2002). Similar findings were also reported by Sun *et al.* (2002), who mentioned that reduction of hydrophilic tendencies was associated with the reduction of free hydroxyl ions of the phenolic groups present in the cellulose and lignin components.

## CONCLUSIONS

1. There was significant improvement in physical and mechanical properties at 5% OPS nanoparticle concentration, which indicated better penetration of PF resin and OPS nanoparticles into IP-OPT.
2. The assessed physical, mechanical, and thermal properties showed their best performances when the OPS nanoparticle concentration was 5%.
3. OPS nanoparticles with PF resin showed better performance compared to PF resin alone.
4. Thus, impregnating IP-OPT with OPS nanoparticles and PF resin may be a good method to improve the physical, mechanical, and thermal properties of IP-OPT.

## ACKNOWLEDGEMENTS

The authors would like to thank Universiti Sains Malaysia (USM), Penang, Malaysia, for providing Research Grant no. RU-1001/PTEKIND/811195. The authors would also like to thank Prof. Pingkan Aditiawati, School of Life Sciences and Technology, Institut Teknologi Bandung, West Java-Indonesia and Prof. Y. S. Hadi, Department of Forest Product, Faculty of Forestry, Bogor Agricultural University, West Java, Indonesia, for providing the necessary facilities for preparing part of the research during a sabbatical leave for the period of December 1, 2011 to August 31, 2012.

## REFERENCES CITED

- Abdul Khalil, H. P. S., Ismail, H., Ahmad, M. N., Ariffin, A., and Hassan, K. (2001). "The effect of various anhydride modification on mechanical properties and water absorption of oil palm fruit bunches reinforced polyester composites," *Polym. Int.* 50(1), 395-402.
- Abdul Khalil, H. P. S., and Rozman, H. D. (2004). "Gentian dan komposit: Lignoselulosik," Pulau Pinang: Penerbit Universiti Sains Malaysia.
- Abdul Khalil, H. P. S., Alwani, M. S., Ridzuan, R., Kamarudin, H., and Khairul, A. (2008). "Chemical composition, morphological characteristics, and cell wall structure of Malaysian oil palm fibres," *J. Polym. Plast. Technol. Eng.* 47(3), 273-280.
- Abdul Khalil, H. P. S., Bhat, A. H., Jawaid, M., Amouzgar, P., Ridzuan, R., and Said, M. R. (2010). "Agro-wastes: Mechanical and physical properties of resin impregnated oil palm trunk core lumber," *Journal of Polymer Composites* 3(4), 638-644.

- Abdul Khalil, H. P. S., Fizree, H. M., Jawaid, M., and Alattas, O. S. (2011). "Preparation and characterization of nano-structured materials from oil palm ash: A bio-agricultural waste from oil palm mill," *BioResources* 6(4), 4537-4546.
- Abdul Khalil, H. P. S., Amouzgor, P., Jawaid, M., Hassan, A., Ahmad, F., Hadiyane, A., and Dungani, R. (2012). "New approach to oil palm trunk core lumber material properties enhancement via resin impregnation," *Journal of Biobased Material and Bioenergy* 6(3), 1-10.
- Abdullah, C. K. (2010). "Impregnation of oil palm trunk lumber (OPTL) using thermoset resins for structural applications," MS Thesis, Universiti Sains Malaysia.
- Amin, M. R. M., and Abdul Khalil, H. P. S. (2004). "Agro-Lumber: Utilization of oil palm trunk for new lumber material," in: *Proceedings of the 3rd USM-JIRCAS Joint International Symposium*, Penang, Malaysia, pp. 272-276.
- Anwar, U. M. K., Paridah, M. T., Hamdan, H., Sapuan, S. M., and Bakar, E. S. (2009). "Effect of curing time on physical and mechanical properties of phenolic-treated bamboo strips," *Ind. Crops Prod.* 29(1), 214-219.
- Arami-Niya, A., Wan Daud, W. M. A., and Mjalli, F. S. (2010). "Using granular activated prepared from oil palm shell by  $ZnCl_2$  and physical activation for methane adsorption," *Journal of Analytical and Applied Pyrolysis* 89(2), 197-203.
- ASTM-D256. (2006). *Standard Test Methods for Determining the Izod Pendulum Impact Resistance of Plastics*, ASTM International, West Conshohocken, PA.
- ASTM-D790. (2003). *Standard Test Methods for Flexural Properties of Unreinforced and Reinforced Plastics and Electrical Insulating Materials*, ASTM International, West Conshohocken, PA.
- ASTM-D3039. (2000). *Standard Test Method for Tensile Properties of Polymer Matrix Composite Materials*, ASTM International, West Conshohocken, PA.
- Bakar, E. S., Rachman, O., Hermawan, D., Karlinasari, L., and Rosdiana, N. (1998). "Utilization of oil palm trunk (*Elaeis guineensis* Jacq) as construction materials and furniture (I): Physical, chemical and natural durability properties of oil palm wood," *Journal of Forest Products Technology* 11(1), 1-11 (in Indonesian).
- Bakar, E. S., Rachman, O., Darmawan, W., and Hidayat, I. (1999a). "Utilization of oil palm trunk (*Elaeis guineensis* Jacq) as construction materials and furniture (II): Mechanical properties of oil palm wood," *Journal of Forest Products Technology* 12(1), 10-20 (in Indonesian).
- Bakar, E. S., Massijaya, Y., Tobing, T.L., and Ma'mur, A. (1999b). "Utilization of oil palm trunk (*Elaeis guineensis* Jacq) as construction materials and furniture (III): Treatability properties of oil palm wood with Basilite-CFK and Impralite-BL," *Journal of Forest Products Technology* 12(2), 13-20 (in Indonesian).
- Bakar, E. S., Paridah, Md. T., Fauzi, F., Mohd Hamami, S., and Tang, W. C. (2008). "Properties enhancement of oil palm lumber through modified compreg method: A comprehensive solution to oil palm wood properties flaws," in: *Proceedings of the 7<sup>th</sup> National Seminar on the Utilization of Oil Palm Tree, Malaysia: Oil Palm Tree Utilization Committee (OPTUC)*, Kuala Lumpur, pp. 99-112.
- Bhat, I. H., Abdullah C. K., Abdul Khalil, H. P. S., Ibrahim, M. H., and Fazita, M. R. N. (2010). "Properties enhancement of resin impregnated agro waste: Oil palm trunk lumber," *Journal of Reinforced Plastics and Composites* 29(22), 3301-3308.
- Bhat, A. H., and Abdul Khalil, H. P. S. (2011). "Exploring "nano filler" based on oil palm ash in polypropylene composites," *BioResources* 6(2), 1288-1297.

- Brown, S. K. (1980). "Mechanism of fracture in filled thermosetting resins," *The British Polymer Journal* 12(1), 24-30.
- Chen, H., Miao, M., and Ding, X. (2009). "Influence of moisture absorption on the interfacial strength of bamboo/vinyl ester composites," *Comp. Part A* 40(12), 2013-2019.
- Deka, M., and Saikia, C. N. (2000). "Chemical modification of wood with thermosetting resin: Effect on dimensional stability and strength property," *Bioresource Technology* 73(2), 179-181.
- Deka, M., Das, P., and Saikia, C. N. (2003). "Studies on dimensional stability, thermal degradation and termite resistant properties of bamboo (*Bambusa tulda* Roxb.) treated with thermosetting resin," *Bamboo Rattan* 2(1), 29-41.
- Dhakal, M., Zhang, Z. Y., and Richardson, M. O. W. (2007). "Effect of water absorption on the mechanical properties of hemp fibre reinforced unsaturated polyester composites," *Compos. Sci. Technol.* 67(7-8), 1674-1683.
- Dungani, R., Jawaid, M., Abdul Khalil, H. P. S., Jasni, Aprilia, S., Hakeem, K. R., Hartati, S., and Islam, M. N. (2013a). "A review on quality enhancement of oil palm trunk waste by resin impregnation: Future materials," *BioResources* 8(2), 3136-3156.
- Dungani, R., Islam, Md. N., Abdul Khalil, H. P. S., Hartati, S., Abdullah, C. K., Dewi, M., and Hadiyane, A. (2013b). "Termite resistance study of oil palm trunk lumber (OPTL) impregnated with oil palm shell meal and phenol-formaldehyde resin," *BioResources* 8(4), 4937-4950.
- Erwinsyah. (2008). "Improvement of oil palm wood properties using bioresin," PhD dissertation, Institut für Forstnutzung und Forsttechnik, Dresden: Fakultät für Forst-, Geo- und Hydrowissenschaften, Technische Universität Dresden.
- Guo, J., and Lua, A. C. (2002). "Characterization of adsorbent prepared from oil-palm shell by CO<sub>2</sub> activation for removal of gaseous pollutant," *Materials Letters* 55(5), 334-339.
- Hartono, R. (2012). "Quality enhancement of oil palm trunk of inert part by close system compression method and compregnation phenol formaldehyde," PhD dissertation, Bogor Agricultural University, School of Postgraduate, Bogor Agricultural University (in Indonesian).
- Hu, R. H., Sun, M. Y., and Lim, J. K. (2010). "Moisture absorption, tensile strength and microstructure evolution of short jute fibre/poly lactide composite in hydrothermal environment," *Mater. Design* 31(7), 3167-3173.
- Ibach, R. E., and Ellis, W. D. (2005). "Lumen modification," in: *Handbook of Wood Chemistry and Wood Composites*, W. R. M. Rowell (ed.), CRC Press, Boca Raton, pp. 421-445.
- Islam, M. N., Dungani, R., Abdul Khalil, H. P. S., Alwani, M. S., Nadirah, W. O. W., and Fizree, H. M. (2013). "Natural weathering studies of oil palm trunk lumber (OPTL) green polymer composites enhanced with oil palm shell (OPS) nanoparticles," *SpringerPlus* 2: 592.
- Islam, M. S., Rahman, M. R., Jusoh, I., and Ibrahim, N. F. (2010). "Dynamic Young's modulus and dimensional stability of Botai tropical wood impregnated with polyvinyl alcohol," *Journal of Scientific Research* 2(2), 227-236.
- Joseph, P. V., Rabello, M. S., Mattoso, L. H. C., Joseph, K., and Thomas, S. (2002). "Environment effects on the degradation behavior of sisal fibre reinforced polypropylene composites," *Comp. Sci. Technol.* 62(10-11), 1357-1372.

- Killmann, W., and Choon, L. S. (1985). "Anatomy and properties of oil palm stem," *Bulletin PORIM* 11, 18-42.
- Lai, L. W., and Idris, A. (2013). "Disruption of oil palm trunks and fronds by microwave-alkali pretreatment," *BioResources* 8(2), 2792-2804.
- Leong, Y. W., Abu Bakar, M. B., Mohd Ishak, Z. A., Ariffin, A., and Pukanszky, B. (2004). "Comparison of mechanical properties and interfacial interaction between talc, kaolin and calcium carbonate filled polypropylene composites," *J. Appl. Polym. Sci.* 91(5), 3315-3326.
- Lim, S. C., and Khoo, K. (1986). "Characteristics of oil palm trunk and its potential utilization," *The Malaysian Forester* 49(1), 3-22.
- Mahlia, T. M. I., Abdulmiun, M. Z., Alamsyah, T. M. I., and Mukhlisien, D. (2001). "An alternative energy source from palm wastes industry for Malaysia and Indonesia," *Energ. Convers. Manag.* 42(18), 2109-2118.
- Mishra, S., Misra, M., Tripathy, S. S., Nayak, S. K., and Mohanty, A. K. (2001). "Potential of pineapple leaf fibre as reinforcement in PALP-polyester composite: Surface modification and mechanical performance," *J. Reinf. Plast. Compos.* 20(4), 322-334.
- Mishra, S., Naik, J. B., and Patil, Y. P. (2000). "The compatibilising effect of maleic anhydride on swelling and mechanical properties of plant fibre-reinforced novolac compared," *Oil Palm Industry Economic Journal* 3(2), 21-31.
- Mizanur Rahman, M. (2009). "UV-cured henequen fibres as polymeric matrix reinforcement: Studies of physico-mechanical and degradable properties," *Mater. Design* 30(6), 2191-2197
- Park, S., Baker, J., Himmel, M., Parilla, P., and Johnson, D. (2010). "Cellulose crystallinity index: Measurement techniques and their impact on interpreting cellulose performance," *Biotechnology for Biofuels* 3, 10.
- Paul, K. T., Satphaty, S. K., Manna, L., Chakraborty, K. K., and Nando, G. B. (2007). "Preparation and characterization of nano structured materials from fly ash: A waste from thermal power stations, by high energy ball milling," *Nanoscale Res. Lett.* 2(8), 397-404.
- Patterson, A. L. (1939). "The Scherrer formula for X-ray particle size determination," *Physical Review* 56, 978.
- Remiro, P. M., Cortazar, M., Calahorra, E., and Calafel, M. M. (2002). "The effect of crosslinking and miscibility on the thermal degradation of an uncured and an amine-cured epoxy resin blended with poly(epsilon-caprolactone)," *Polymer Degradation and Stability* 78(1), 83-93.
- Seena, J., Sreekala, M. S., Oommen, Z., Koshyc, P., and Sabu, T. (2002). "A comparison of mechanical properties of phenol formaldehyde composites reinforced with banana fibres and glass fibres," *Journal of Composite Science and Technology* 62(14), 1857-1868.
- Shafiq, P., Jumaat, M. Z., and Mahmud, H. (2011). "Oil palm shell as a lightweight aggregate for production high strength lightweight concrete," *Construction and Building Materials* 25(4), 1848-1853.
- Sun, X. F., Sun, R., and Sun, J. X. (2002). "Acetylation of rice straw with or without catalysts and its characterization as a natural sorbent in oil spill cleanup," *Journal of Agricultural and Food Chemistry* 50(22), 6428-6433.

- Yang, H., Yan, R., Chin, T., Liang, D. T., Chen, H., and Zheng, C. (2004).  
“Thermogravimetric analysis-Fourier transform infrared analysis of palm oil waste pyrolysis,” *Journal of Energy and Fuels* 18(6), 1814-1821.
- Zainudin, N. F., Lee, K. T., Komaruddin, A. H., Bhatia, S., and Mohamed, A. R. (2005).  
“Study of adsorbent prepared from oil palm ash (OPA) for fuel gas desulfurization,” *Separation and Purification Technology* 45(1), 50-60.
- Zhang, C., Tjiu, W. W., Liu, T., Lui, W. Y., Phang, I. Y. and Zhang, W. D. (2011).  
“Dramatically enhanced mechanical performance of nylon-6 magnetic composites with nanostructured hybrid one-dimensional carbon nanotube–two-dimensional clay nanoplatelet heterostructures,” *The Journal of Physical Chemistry B* 115(13), 3392-3399.

Article submitted: August 29, 2013; Peer review completed: November 9, 2013; Revised version received and accepted: November 15, 2013; Published: November 25, 2013.